J Mater Sci: Mater Electron (2015) 26:7303–7308
DOI 10.1007/s10854-015-3358-8

A simple sonochemical approach for synthesis of cadmium molybdate nanoparticles and investigation of its photocatalyst application

Saeid Khademolhoseini[1] · Mojtaba Zakeri[2] · Saman Rahnamaeiyan[3] · Mahdi Nasiri[4] · Ruhollah Talebi[1]

Received: 16 May 2015 / Accepted: 12 June 2015 / Published online: 20 June 2015

Abstract Nanoparticles cadmium molybdate was prepared by ultrasonic method using cadmium(II) nitrate hexahydrate and ammonium heptamolybdate tetrahydrate were used as precursor materials. To the best of authors' knowledge, it is the first time that cadmium molybdate was synthesized by ultrasonic method. The as synthesized nanostructures were characterized by X-ray diffraction, scanning electron microscopy, X-ray energy dispersive spectroscopy, and ultraviolet–visible spectroscopy. To evaluate the catalytic properties of nanocrystalline cadmium molybdate, the photocatalytic degradation of 2-naphthol under visible light irradiation was carried out.

1 Introduction

Throughout last decades an important activity in the use of semiconductor oxides as photocatalysts has been observed. Since discovery of photocatalytic activity of TiO_2 by UV irradiation, many works have described novel methods to synthesize photocatalysts with special textural properties in order to increase its photocatalytic activity in redox reactions. Although TiO_2 anatase form isconsidered as the photocatalyst for excellence, different semiconductor oxides such as WO_3, ZnO, and CdS have been proposed for photocatalytic conversion [1–3]. Recently some binary and ternary oxides with scheelite and related structures have shown photocatalytic activity under UV irradiation [4,5]. In particular, $PbMoO_4$ with scheelite structure have gained interest as photocatalyst for the splitting of water into hydrogen and oxygen [6,7] and for the degradation of complex organic compounds [8,9]. For this reason, different soft chemistry methods have been developed to obtain $PbMoO_4$ with specific textural properties and morphology such as co-precipitation [10], hydrothermal [11], microwave irradiation [12], and sonochemical [10–15]. We tried to extend our knowledge to apply the sonochemical technique to synthesize $CdMoO_4$ photocatalyst. The physical phenomenon responsible for the ultrasonic process is acoustic cavitation. The ultrasonic cavitation generates a very strong stirring environment. Therefore, application of ultrasound is expanding in material science for dispersion, emulsifying, crushing, impregnation, surface treatment, synthesis and activation of nanoparticles. During the process, the rapid ultrasonic vibrations and cavitation effects cause to increase collision between the molecules which in turn enhance the chemical reactivity. The photocatalytic degradation was investigated using 2-naphthol under visible light irradiation ($\lambda > 400$ nm). The resulting degradation rates of the 2-naphthol were measured to be as high as 90 % in 360 min. In the current study, the synthesis of $CdMoO_4$ nanoparticles is reported [16–19]. This production is done by ultrasonic solution of cadmium(II) nitrate hexahydrate $Cd(NO_3)_3{\cdot}6H_2O$ and ammonium heptamolybdate tetrahydrate $(NH_4)_6Mo_7O_{24}.4H_2O$. Besides, the effect of reaction parameters ultrasonic power on the morphology and particle size of $CdMoO_4$ nanoparticles was investigated.

✉ Ruhollah Talebi
ruhollahtalebi90@gmail.com

[1] Young Researchers and Elite Club, South Tehran Branch, Islamic Azad University, Tehran, Iran

[2] Young Researchers and Elite Club, Najaf Abad Branch, Islamic Azad University, Isfahan, Iran

[3] Islamic Azad University, Borujerd, Iran

[4] Young Researchers and Elite Club, Borujerd Branch, Islamic Azad University, Borujerd, Iran

2 Experimental

2.1 Materials and characterization

All chemical reagents in this experiment were of analytical grade and used without further purification. X-ray diffraction (XRD) patterns were recorded by a Philips-X'PertPro, X-ray diffractometer using Ni-filtered Cu Kα radiation at scan range of $10 < 2\theta < 80$. Scanning electron microscopy (SEM) images were obtained on LEO-1455VP equipped with an energy dispersive X-ray spectroscopy. Spectroscopy analysis (UV–Vis) was carried out using shimadzu UV–Vis scanning UV–Vis diffuse reflectance spectrometer. Ultrasonic irradiation was accomplished with a high-intensity ultrasonic bath. The EDS analysis with 20 kV accelerated voltage was done.

2.2 Synthesis of $CdMoO_4$ nanoparticles

$CdMoO_4$, was synthesized ultrasonic method. Appropriate amounts of $Cd(NO_3)_3{\cdot}6H_2O$ and ammonium heptamolybdate tetrahydrate ($(NH_4)_6Mo_7O_{24}.4H_2O$) were used as the Zn and Mo sources. In a typical synthesis (0.116 g) ammonium heptamolybdate tetrahydrate and (0.202 g) of $Cd(NO_3)_3{\cdot}6H_2O$ were dissolved in 30 ml distilled water and methanol, respectively. Then $Cd(NO_3)_3{\cdot}6H_2O$ was heated at 60 °C for 10 min and finally the ammonium heptamolybdate tetrahydrate solution was added dropwise to this solution with pH 5–6 and solution was heated at 45 °C and finally treated with ultrasonic irradiation with different power. The white product was filtered, washed with distilled water and ethanol several times and dried in vacuum in less than 90 °C. Finally, the product was dried in vacuum at 90 °C for 2 h. Reaction conditions are listed in Table 1.

Table 1 Reaction conditions for $CdMoO_4$ nanoparticles

Sample no	Power (W)	Time (min)
1	50	30
2	70	30
3	90	30

2.3 Photocatalytic experimental

The 2-naphthol photodegradation was examined as a model reaction to evaluate the photocatalytic activities of the $CdMoO_4$ nanoparticles. The photocatalytic experiments were performed under an irradiation wavelength of $\lambda > 400$ nm. The photocatalytic activity of nanocrystalline cadmium molybdate obtained from sample no. 4 was studied by the degradation of 2-naphthol solution as a target pollutant. The photocatalytic degradation was performed with 0.001 g of 2-naphthol solution containing 0.1 g of $CdMoO_4$. This mixture was aerated for 30 min to reach adsorption equilibrium. Later, the mixture was placed inside the photoreactor in which the vessel was 15 cm away from the visible source of 400 W Xeno lamp. The photocatalytic test was performed at room temperature. Aliquots of the mixture were taken at definite interval of times during the irradiation, and after centrifugation they were

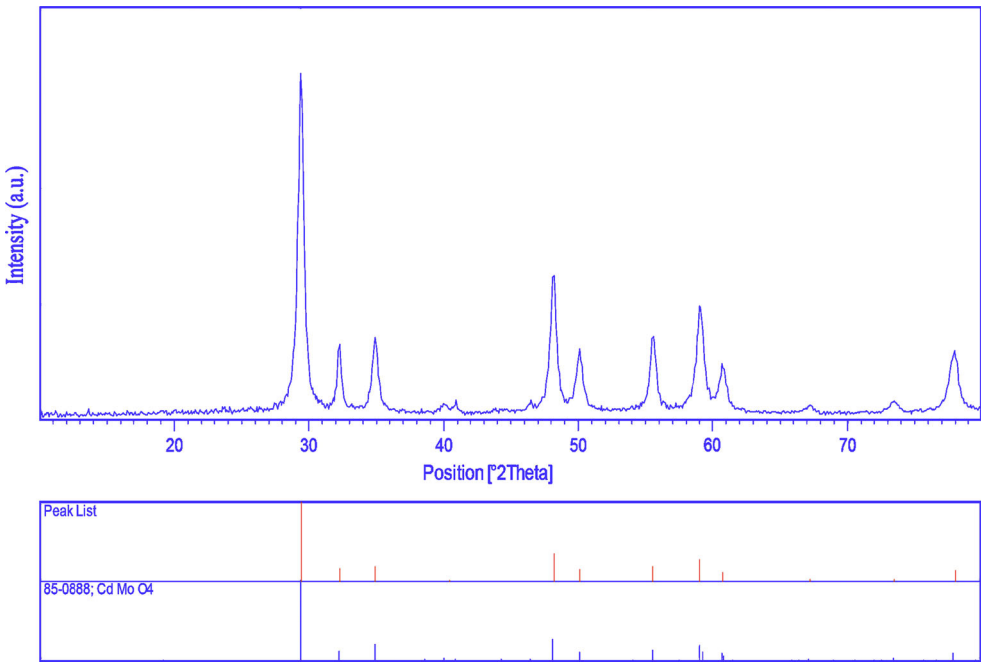

Fig.1 XRD pattern of $CdMoO_4$ nanoparticles (sample no. 1)

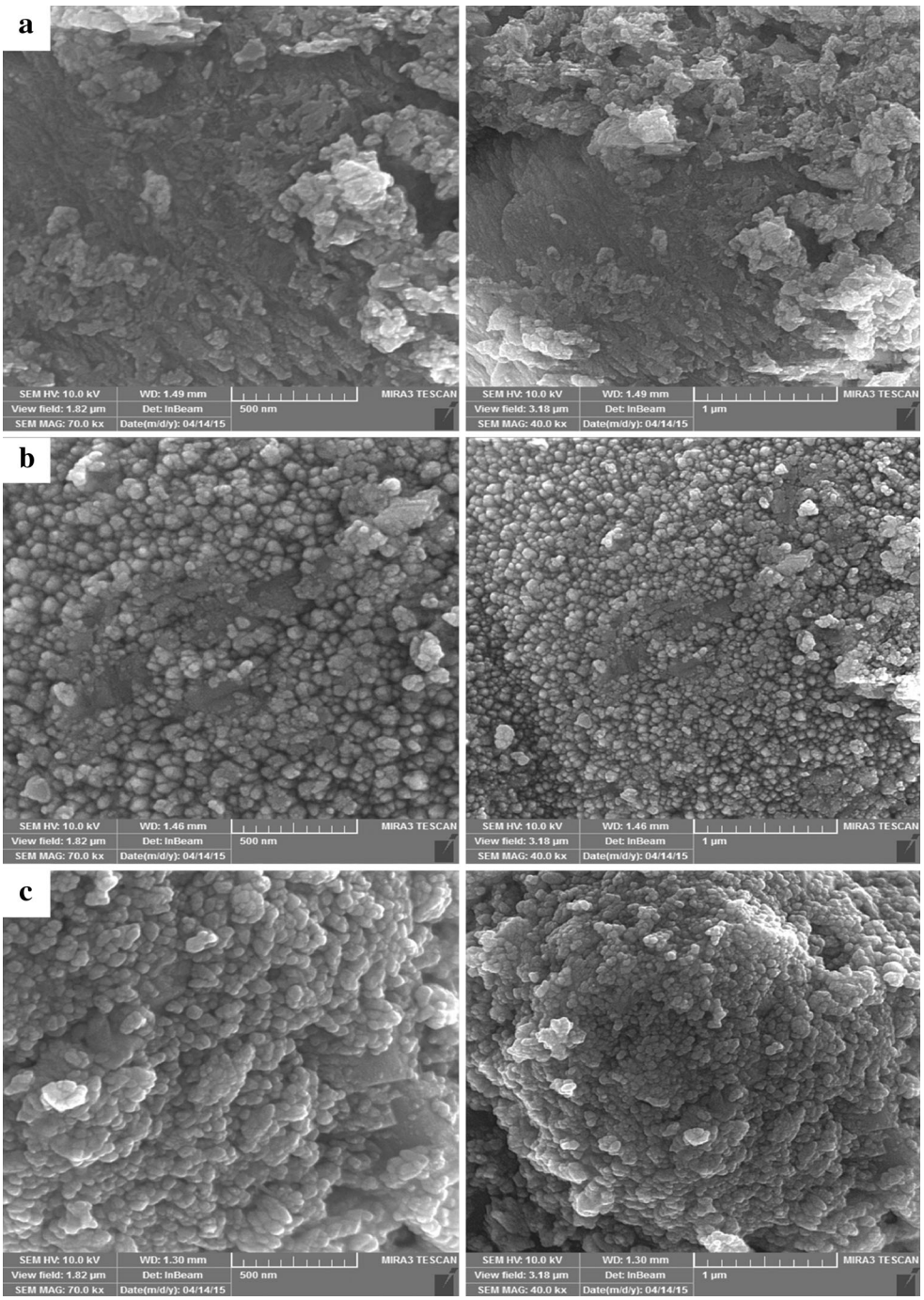

Fig.2 SEM images of $CdMoO_4$ nanoparticles, **a** sample no. 1, **b** sample no. 2, **c** sample no. 3

analyzed by a UV–vis spectrometer. The 2-naphthol degradation percentage was calculated as:

$$\text{Degradation rate } (\%) = \frac{A0 - A}{A} \times 100$$

where A_0 and A are the absorbance value of solution at A_0 and A min, respectively.

3 Results and discussion

Figure 1 shows a typical XRD pattern ($10° < 2\theta < 80°$) of $CdMoO_4$ nanoparticles (sample 1). Based on the Fig. 1, the diffraction peaks can be indexed to pure tetragonal phase of $CdMoO_4$ (space group *I41/a*, JCPDS No. 85-0888). No other crystalline phases were detected. From XRD data, the

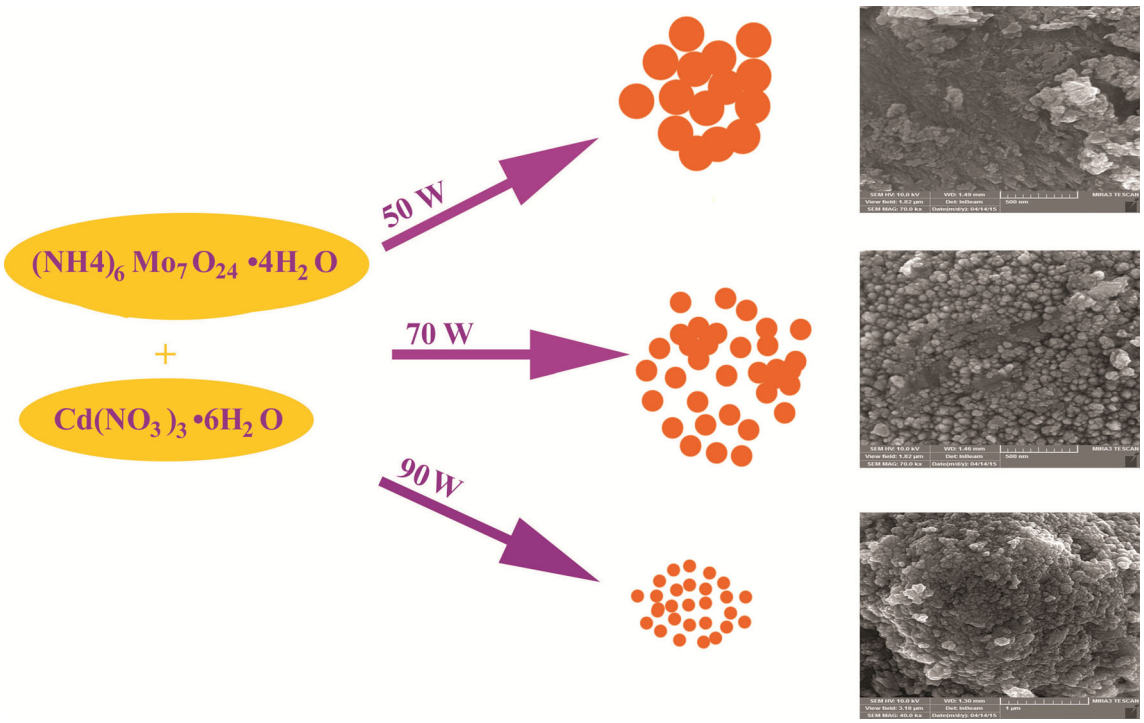

Scheme 1 The effect of power on morphology of products

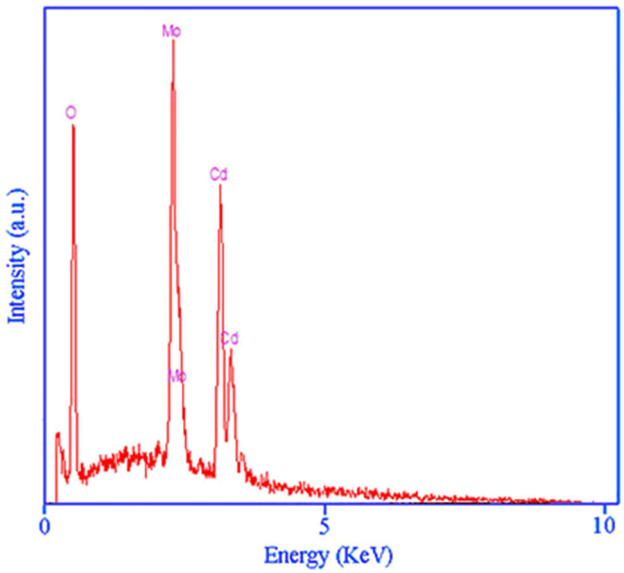

Fig.3 EDS pattern of $CdMoO_4$ nanoparticles (sample no 2)

crystallite diameter (D_c) of $CdMoO_4$ nanoparticles obtained from sample 1 was calculated to be 45 nm using the Scherer equation:

$$D_c = K\lambda/\beta\cos\theta \quad \text{Scherer equation}$$

where β is the breadth of the observed diffraction line at its half intensity maximum (400), K is the socalled shape factor, which usually takes a value of about 0.9, and λ is

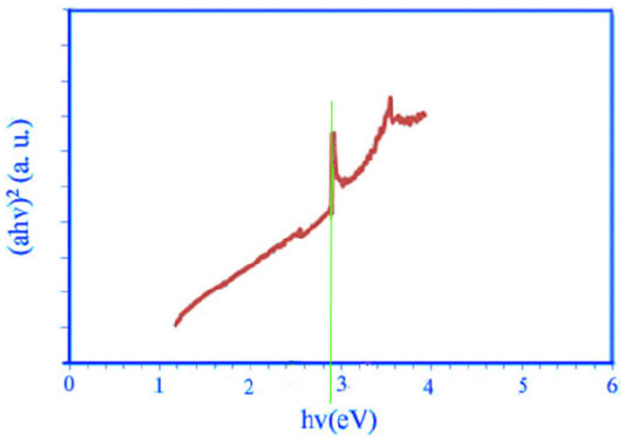

Fig.4 UV–Vis pattern of $CdMoO_4$ nanoparticles (sample no 2)

the wavelength of X-ray source used in XRD. The effect of different dosage of sucrose and ultrasonic power on the morphology and particle size of $CdMoO_4$ nanoparticles was investigated. Figure 2a–c shows the SEM images of $CdMoO_4$ nanoparticles sample No 1–3, respectively. Base on the Fig. 2a, the product is mainly composed of the agglomeration nanoparticles. When ultrasonic power increased from 50 to 70 W, morphology of $CdMoO_4$ is consist of agglomeration nanoparticle, as shown in Fig. 2b, respectively. Furthermore, increase in ultrasonic power result in increase size of product. Schematic diagram of formation of nanostructures is illustrated in Scheme 1.

The EDS analysis measurement was used to investigate the chemical composition and purity of $CdMoO_4$ nanoparticles (sample 2, Fig. 3). According to the Fig. 4, the product consists of Cd, Mo, and O elements. Furthermore, neither N nor C signals were detected in the EDS spectrum, which means the product is pure and free of any surfactant or impurity. To investigate the optical properties of the nanocrystalline $CdMoO_4^-$, UV–vis spectra was recorded. Figure 4 shows the UV–vis diffuse reflectance spectrum of sample no 2. Using Tauc's formula, the band gap can be obtained from the absorption data. The energy gap (Eg) of the nanocrystalline $CdMoO_4$ has been estimated by extrapolating the linear portion of the plot of $(\alpha h\nu)^2$ against $h\nu$ to the energy axis. The Eg value of the nanocrystalline $CdMoO_4$ calculated to be 2.85 eV. Photodegradation of methyl orange under UV light irradiation (Fig. 5a–c) was employed to evaluate the photocatalytic activity of the as-synthesized $CdMoO_4$ (sample no. 2). No methyl orange was practically broken down after 6 h without using visible light irradiation or nanocrystalline $CdMoO_4$. This observation indicated that the contribution of self-degradation was insignificant. The probable mechanism of the photocatalytic degradation of 2-naphthol can be summarized as follows:

$$CdMoO_4 + h\nu \rightarrow CdMoO_4^* + e^- + h^+$$

$$h^+ + H_2O \rightarrow OH^{\cdot}$$

$$e^- + O_2 \rightarrow O_2^{\cdot -}$$

$$OH^{\cdot} + O_2^{\cdot -} + \text{2-naphthol} \rightarrow \text{Degradation products}$$

Using photocatalytic calculations by Eq. (1), the 2-naphthol degradation was about 90 % after 6 h irradiation of visible light, and nanocrystalline $CdMoO_4$ presented high photocatalytic activity (Fig. 5a). The spectrofluorimetric time-scans of 2-naphthol solution illuminated at 365 nm with nanocrystalline $CdMoO_4$ are depicted in Fig. 5b. Figure 5b shows continuous removal of 2-naphthol on the $CdMoO_4$ under visible light irradiation. It is generally accepted that the heterogeneous photocatalytic processes comprise various steps (diffusion, adsorption, reaction, and etc.), and suitable distribution of the pore in the catalyst surface is effective and useful to diffusion of reactants and products, which prefer the photocatalytic reaction. In this investigation, the enhanced photocatalytic activity can be related to appropriate distribution of the pore in the sponge-like nanocrystalline $CdMoO_4$ surface, high hydroxyl amount and high separation rate of charge carriers (Fig. 5c).

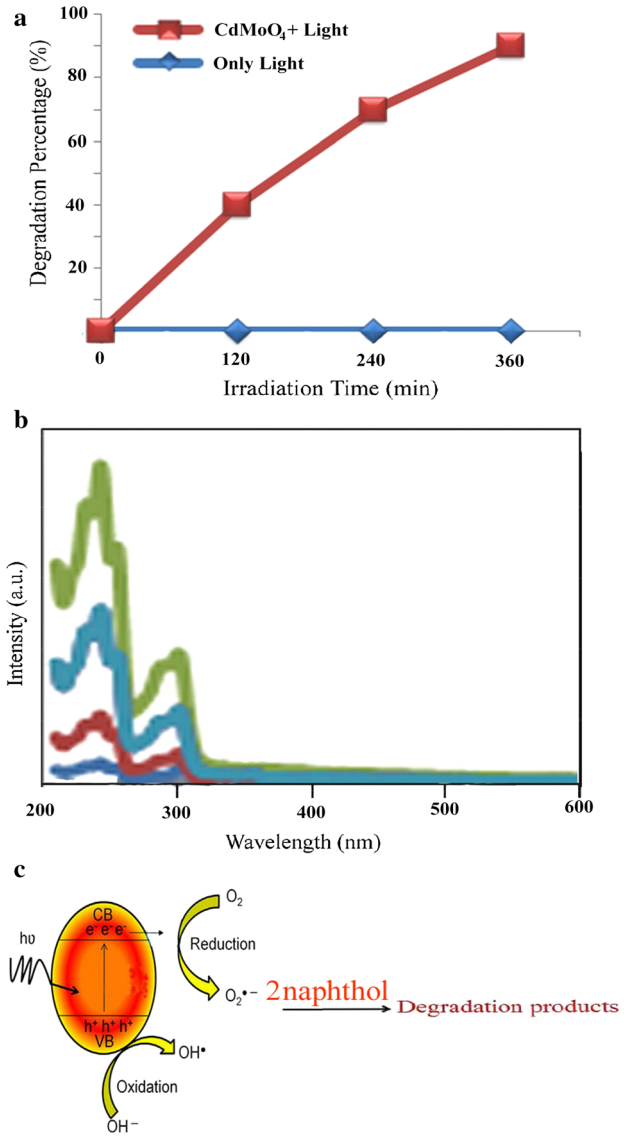

Fig.5 Photocatalytic 2-naphthol degradation of $CdMoO_4$ nanoparticles obtained from sample no. 2 under visible light (**a**), fluorescence spectral time scan of 2-naphthol illuminated at 365 nm with $CdMoO_4$ nanoparticles (**b**), and reaction mechanism of 2-naphthol photodegradation over $CdMoO_4$ under visible light irradiation

4 Conclusions

$CdMoO_4$ nanoparticles have been successfully synthesized through an ultrasonic method. We investigated the effect of dosage of ultrasonic power on the morphology and particle size of $CdMoO_4$ nanoparticles. SEM results indicated that the size and morphology of the products could were found to be greatly influenced by the aforementioned parameters. $CdMoO_4$ nanoparticles were characterized by XRD, UV–Vis, EDS, and SEM. When as prepared nanocrystalline cadmium molybdate was utilized as photocatalyst, the percentage of 2-naphthol degradation was about 90 % after 360 min irradiation of visible light.

Acknowledgments Authors are grateful to council of University of South Tehran for providing financial support to undertake this work.

Conflict of interest The author declares that the research was conducted in the absence of any commercial or financial relationships that could be construed as a potential conflict of interest

References

1. S. Gupta, M. Tripathi, High Energy Chem. **46**, 1 (2012)
2. X.S. Yang, H. Kim, Appl. Mech. Mater. **110**, 3781 (2012)
3. D. Sanchez-Martinez, A. Martinez-de la Cruz, E. Lopez-Cuellar, Solid State Sci. **12**, 60 (2010)
4. Z. Shan, Y.W.H. Ding, F. Huang, J. Mol. Catal. A Chem. **302**, 54 (2009)
5. H. Kato, N. Matsudo, A. Kudo, Chem. Lett. **33**, 1216 (2004)
6. Y. Shimodaira, H. Kato, H. Kobayashi, A. Kudo, Chem. Soc. Jpn. **80**, 885 (2007)
7. A. Kudo, M. Steinberg, A.J. Bard, A. Campion, M.A. Fox, T.E. Mallouk, S.E. Webber, J.M. White, Catal. Lett. **5**, 61 (1990)
8. J. Bi, L. Wu, Y. Zhang, Z. Li, J. Li, X. Fu, Appl. Catal. B Environ. **91**, 135 (2009)
9. G.J. Xing, R. Liu, C. Zhao, Y.L. Li, Y. Wang, G.M. Wu, Ceram. Int. **37**, 2951 (2011)
10. W.S. Wang, L. Zhen, C.Y. Xu, W.Z. Shao, Z.L. Chen, J. Alloys Compd. **529**, 17 (2012)
11. D. Li, Y.F. Zhu, Cryst. Eng. Commun. **14**, 1128 (2012)
12. L.R.N. Hou, L. Lian, L. Zhang, J.Y. Li, Mater. Lett. **109**, 306 (2013).
13. H.W. Liu, L. Tan, Ionics. **16**, 57 (2010)
14. D. Zhu, K. Ki, X. Chen, T. Ying, J. Optoelectron. Adv. Mater. **5**, 403 (2011)
15. Q.L. Dai, G.G. Zhang, P. Liu, J. Wang, J.K. Tang, Inorg. Chem. **51**, 9232 (2012)
16. J. Lin, Z. Zeng, Q. Wang, Inorg. Chim. Acta **408**, 59 (2013)
17. D.B. Hernandez-Uresti, l.C.A. Martinez-de, L.M. Torres-Martinez, Res. Chem. Intermed. **38**, 817 (2012)
18. T.H. Kim, V. Rodríguez-González, G. Gyawali, S.H. Cho, T. Sekino, S.W. Lee, Catal. Today **9**, 14 (2012)
19. A. Sun, D. Wang, Z. Wu, X. Zan, J. Alloys Compd. **505**, 588 (2010)